Searching for ALP DM under strong gravitational lenses

Yuko Urakawa (KEK, iPNS)

w/ A. Basu (Thuringian State Observatory, Tautenburg),

J. Goswami, D. Schwarz (Bielefeld U.)

ALP dark matter

✗

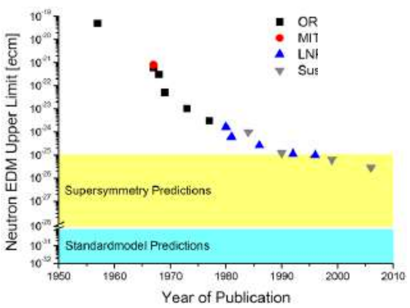

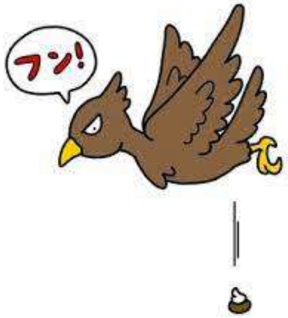

like
particle

✓

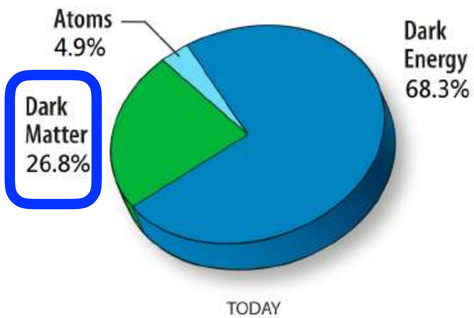

Axion/ALP search

coupling

large small

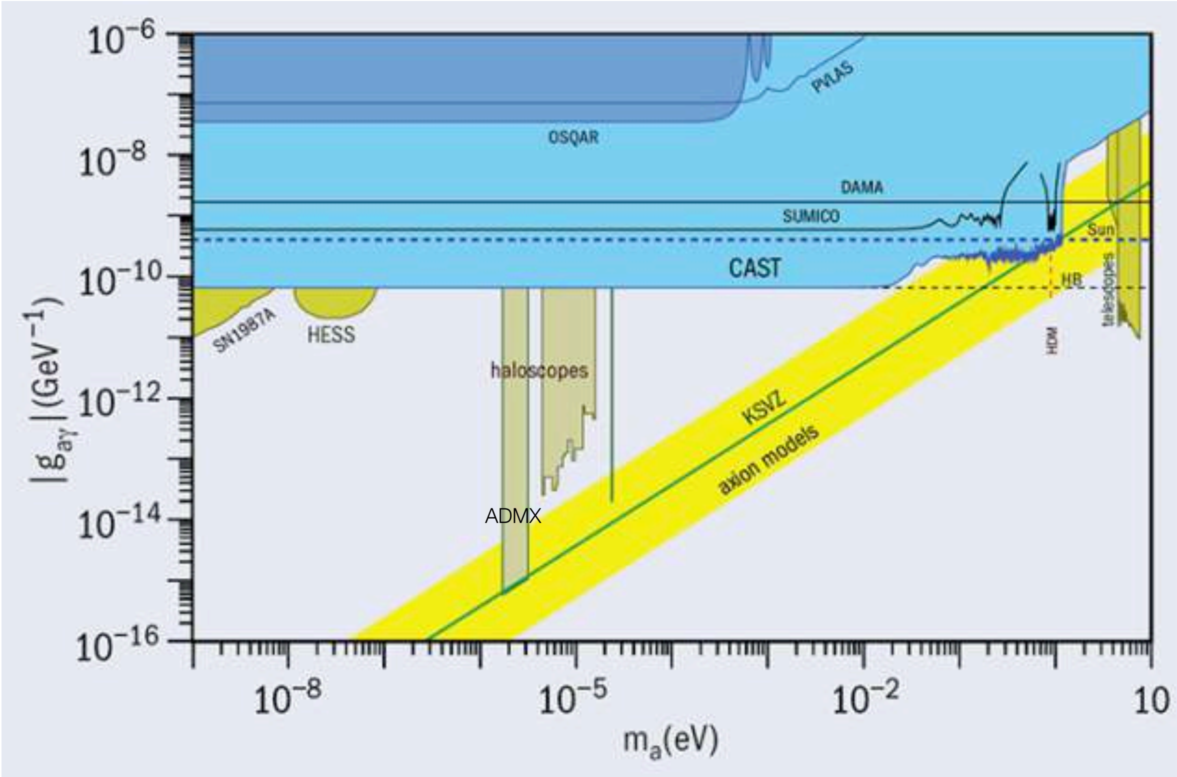

small large

f_a

$$m_a \sim \frac{F_\pi m_\pi}{f_a} \sim \mu\mathrm{eV}\frac{10^{-12}\mathrm{eV}}{f_a}$$

from CAST collaboration

$$g_{a\gamma} \equiv \alpha_{\mathrm{EM}}/(2\pi f_a)$$

generation

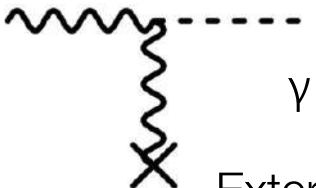

detection

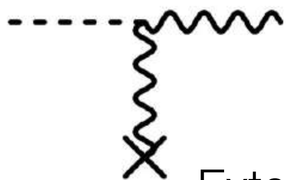

Primakov effect

$\gamma \rightarrow \phi$

$\phi \rightarrow \gamma$

e.g CAST solar plasma

External B or E

External B or E

String axiverse

Superstring theory in compact 6D

Arvanitaki et al. (09, 10), ...

↓

4D low energy EFT + Axions + Moduli ....

Wide mass ranges → Probe of exDim

$$m_a^2 \sim \frac{\mu^4}{f_a^2} e^{-\#\sigma_i}$$

↓

Inflaton, DM candidate (Fuzzy DM)

Hu et al.(00), ...

ex. Large Volume Scenario *Conlon et al. (05)*

Thraxions *Hebecker + (18)*

→ Predicts extremely light axions

Ultra-light axion (DM) search

Astrophysical bodies provide a good probe of ULA DM

$$T = \frac{2\,\pi}{m_{\rm a}} \approx 4 \times 10^{7}\,{\rm s}\left(\frac{10^{-22}\,{\rm eV}}{m_{\rm a}}\right)$$

We need to take into account …

- Model dependence of astrophysical bodies
- Other contaminations
- Calibration error etc..

X-ray observation

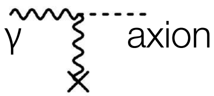

cluster B

Credit; J.Conlon

modulation in X-ray spectrum due γ-a conv.

$$m_a \leq 10^{-13\sim-12}\mathrm{eV} \qquad g_{a\gamma} \leq \mathcal{O}(1) \times 10^{-12}\mathrm{GeV}^{-1}$$

AGN of Hydra A cluster — *Wouters & Brun (13)*

AGN NGC in Perseus cluster — *Berg et al. (16)*

AGN M87 in Virgo cluster — *Marsh et al. (17)*

* ALP does not have to be DM

Depends on

- Exact configuration of B-field along the γ path
- Modeling of emission mechanism

Birefringence

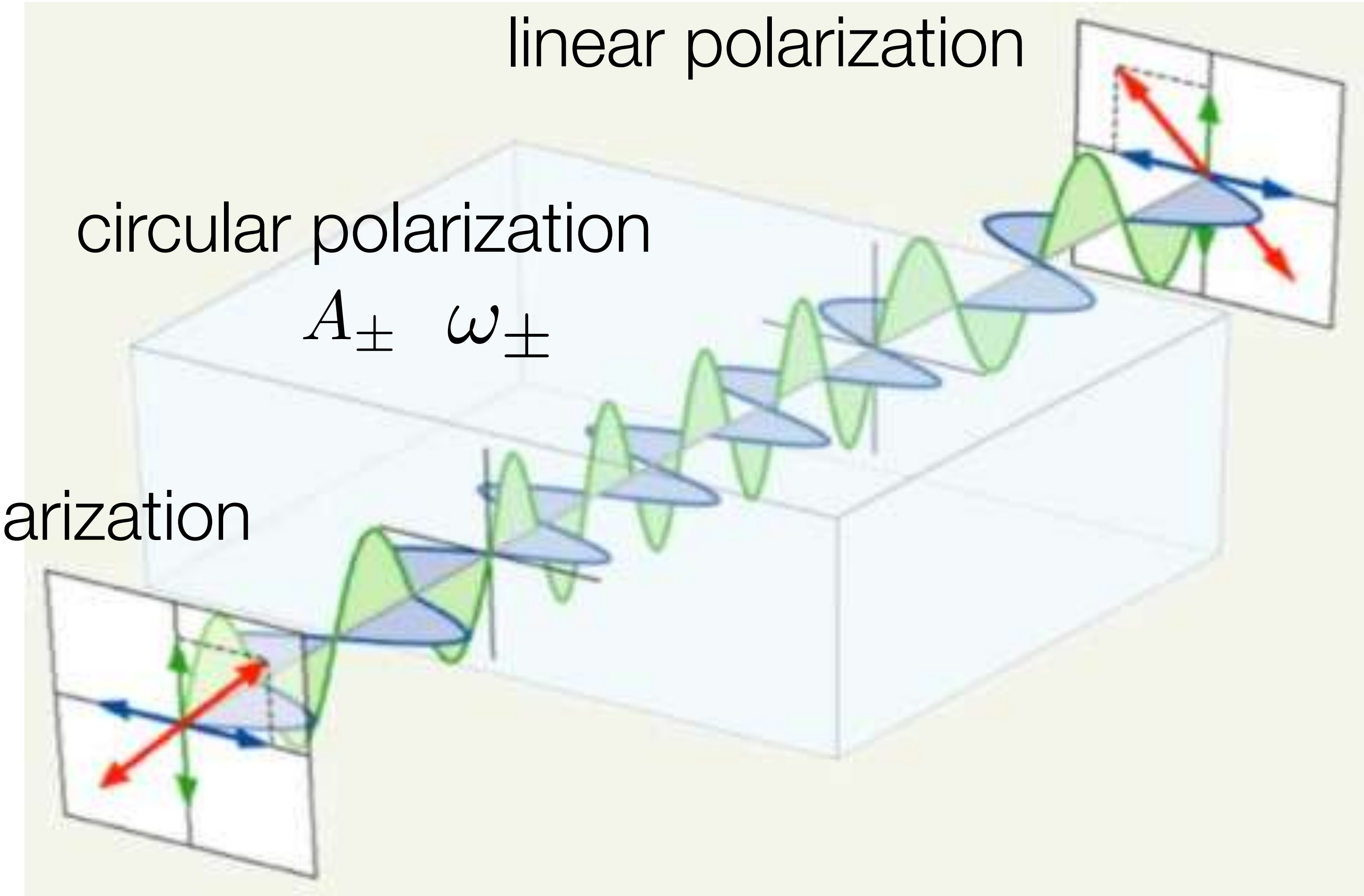

Rotation

Birefringence due to ALP dark matter

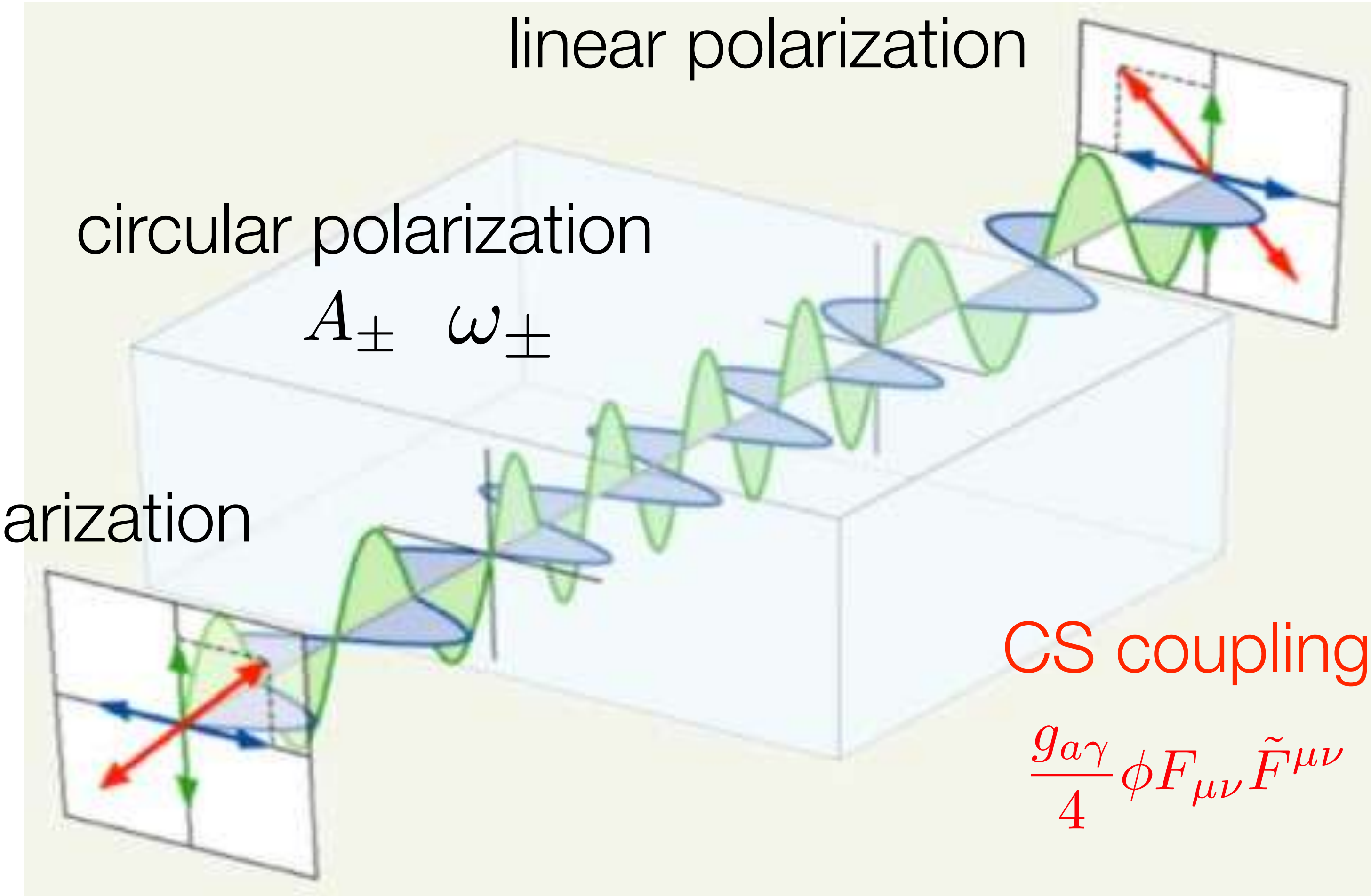

Rotation

Inhomogeneous patches
(k/m >> 1)

$$\Delta\theta_a = \frac{g_{a\gamma}}{2}\left[\phi(t_{\rm obs}, x^i_{\rm obs}) - \phi(t_{\rm em}, x^i_{\rm em})\right]$$

Harari & Sikivie (1992)

Cosmic birefringence due to ALP dark matter

- Cosmic Microwave Background

Fedderke et al. (19), BICEP/Keck collaboration (20)

$$g_{a\gamma} \leq \mathcal{O}(1) \times (10^{-11}\mathrm{GeV}^{-1})\, m/(10^{-21}\mathrm{eV})$$

Limited by calibration / CV(Washout) See also *Minami and Komatsu (20)*

- AGN emission going through axion cloud *Plascencia and Urbano (17)*
- Jet of AGN *Ivanov et al. (18)*
- Protoplanetary disks *Fujita et al. (18)*
- Pulsar *Liu et al. (19)*

Limited by astrophysical modeling, angle calibration,…

Ultra-light ALP DM search through lensed AGN

w/ Basu (Thuringian State Observatory, Tautenburg),

Goswami, Schwarz (Bielefeld U.)

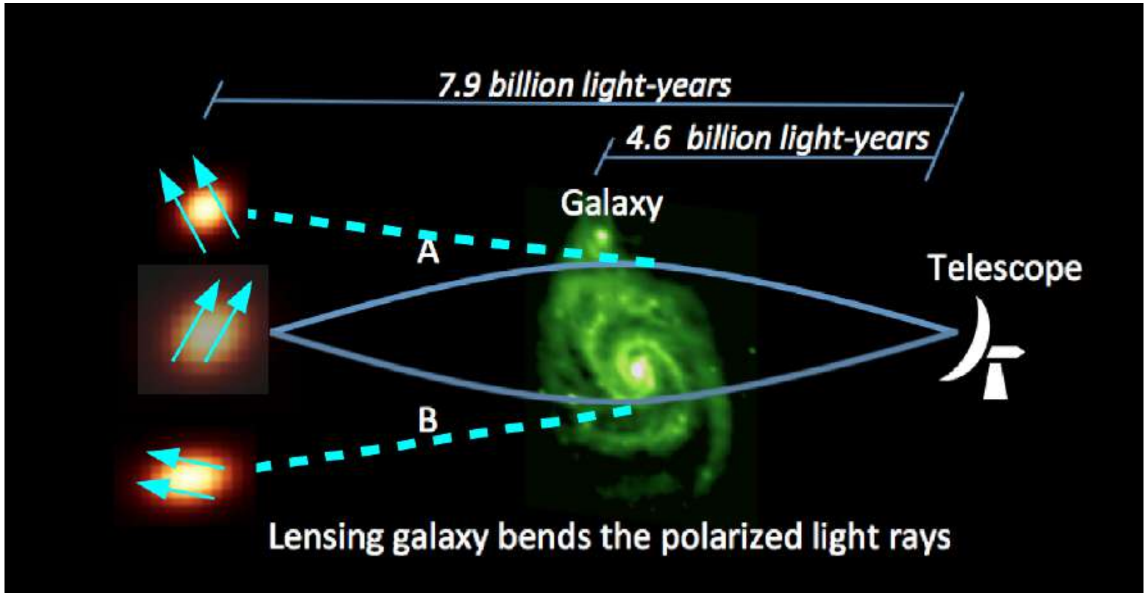

Active galactic Nuclei (AGN)

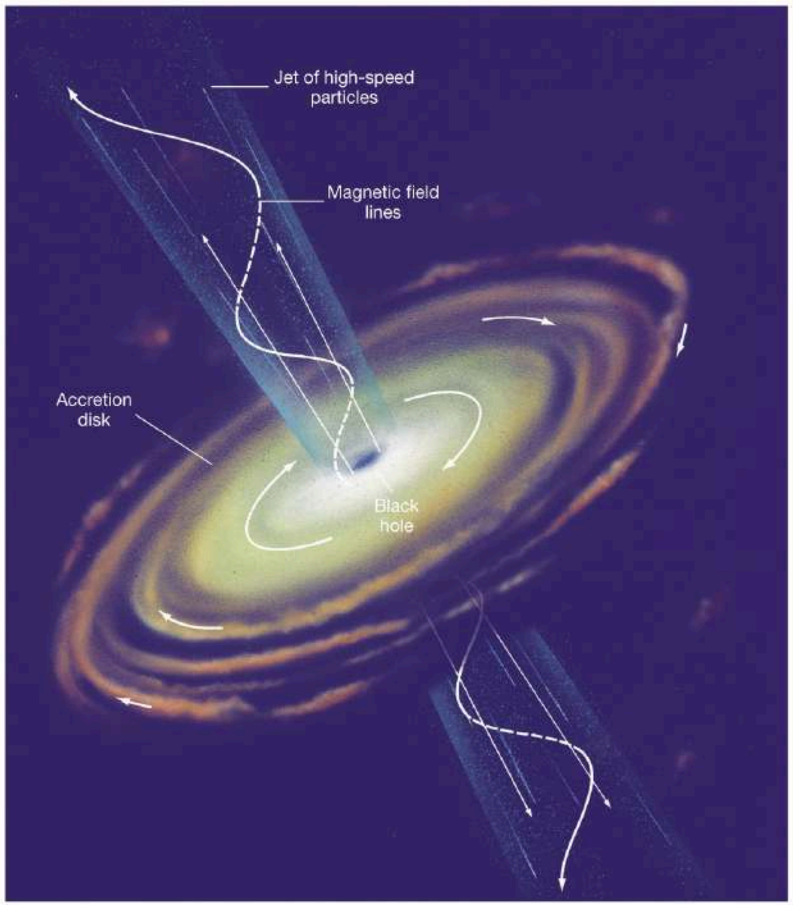

- Efficient particle accelerators
- Relativistic jets
  (w/magnetic field lines)
- Non-thermal emission
- Unified picture of blazer, quasar, radio galaxy

Emission from AGN jet

Fermi-LAT collaboration (11)

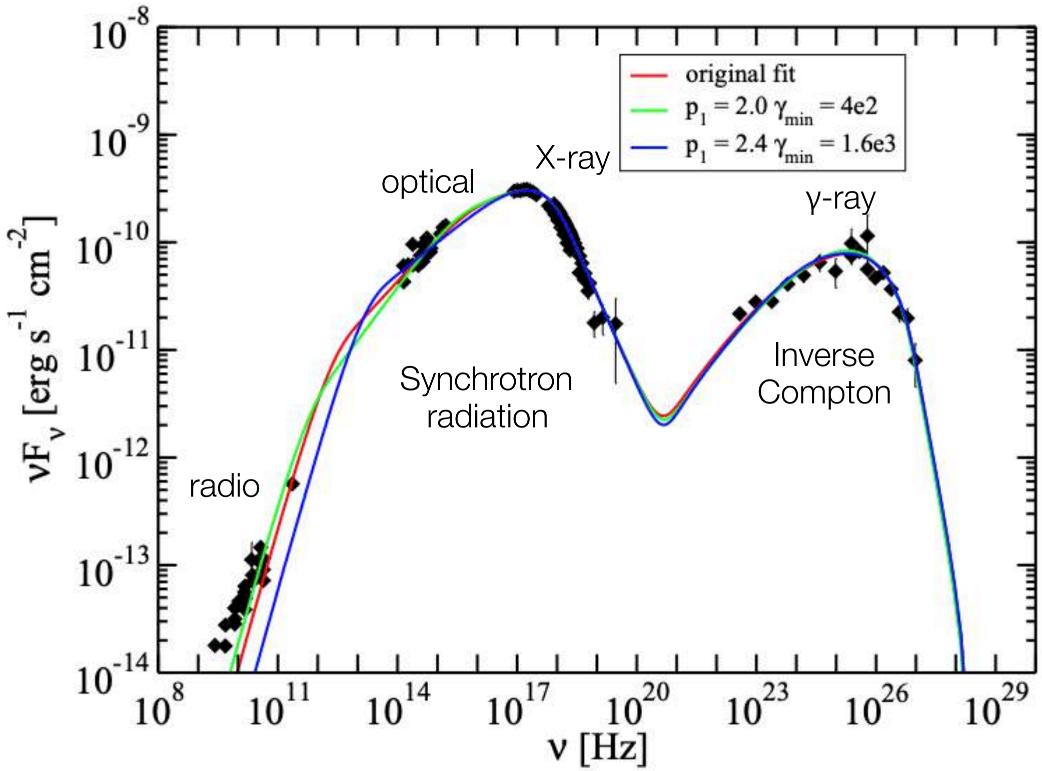

Fig. 12.— SSC model fit of the SED from Mrk421 presented in Figure 11 (for t_{var} ~1 day), with variations by a factor of 2 of the parameter γ_{min}, together with adjustments in the parameter p_1 in order to match the experimental data. See text for further details.

Radio band is dominated by synchrotron radiation.

Synchrotron radiation

Relativistic e$^-$ ($\gamma >> 1$) moving perpendicular to B

$$\gamma \equiv \frac{1}{\sqrt{1-v^2/c^2}}$$

$\longrightarrow$ Acceleration due to Lorentz force $\longrightarrow$ Synchrotron radiation

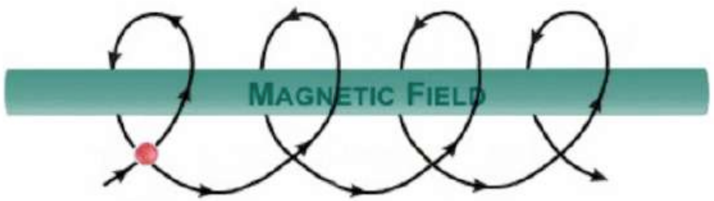

- For $\gamma >> 1$, the emission pattern is sharply collimated forward.
  (peaked in the direction of velocity)

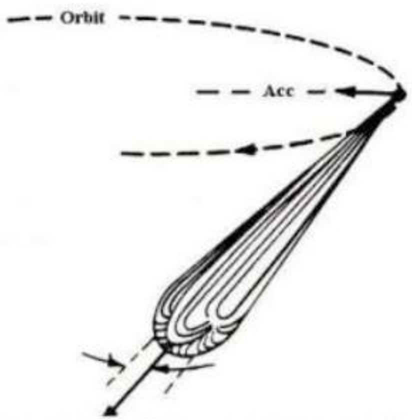

Cone aperture ~ 1/γ

- Emitted photons are polarized.

Radio emission from AGN is polarized.

✔ Necessary to measure birefringence

Radio telescopes (under operation)

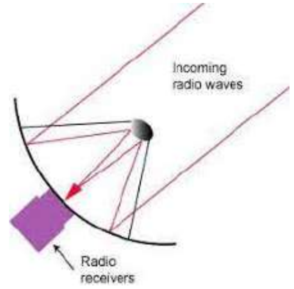

<u>Karl G. Jansky Very Large Array (JVLA)</u> @Socorro, New Mexico

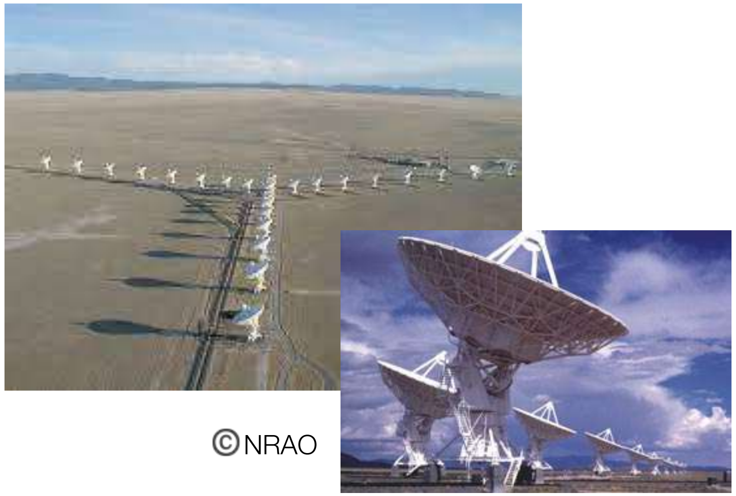

27 antennas arranged in Y-shape

→ Effective aperture up to ~ 36km

- Frequency: 1.0GHz - 50 GHz
- Resolution: 0.04 - 0.2 arcsec

<u>Very Long Baseline Array (VLBA)</u>

10 dishes w/max baseline ~ 8,600km

- Frequency: 0.3GHz - 96 GHz
- Resolution: 0.17 - 22 milliarcsec

ALP search via AGN

Observed rotation angle

$$\theta_0 = \theta_{\rm qso} + \Delta\,\theta_{\rm a} + \delta\,\theta_{\rm cal}$$

intrinsic calibration

birefringence due to ALP

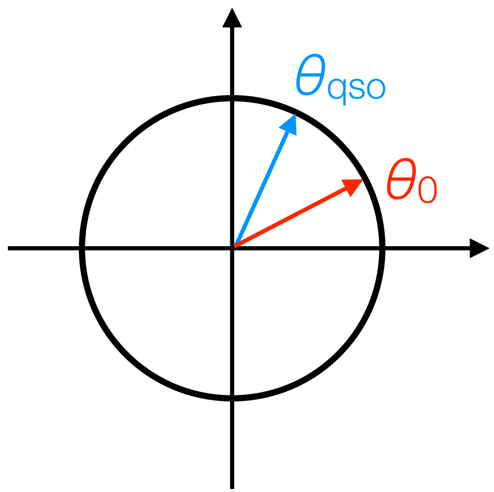

$\theta_{\rm qso}$: Astrophysical assumptions and modeling

$\delta\theta_{\rm cal}$: Stable instrument over year time-scale

$$T = \frac{2\,\pi}{m_{\rm a}} \approx 4 \times 10^7\,{\rm s}\left(\frac{10^{-22}\,{\rm eV}}{m_{\rm a}}\right)$$

* VLA, VLBA (, SKA) are stable at best several weeks.

\+ Typical angle calibration error (~1–5 degrees)

Strong gravitational lensing

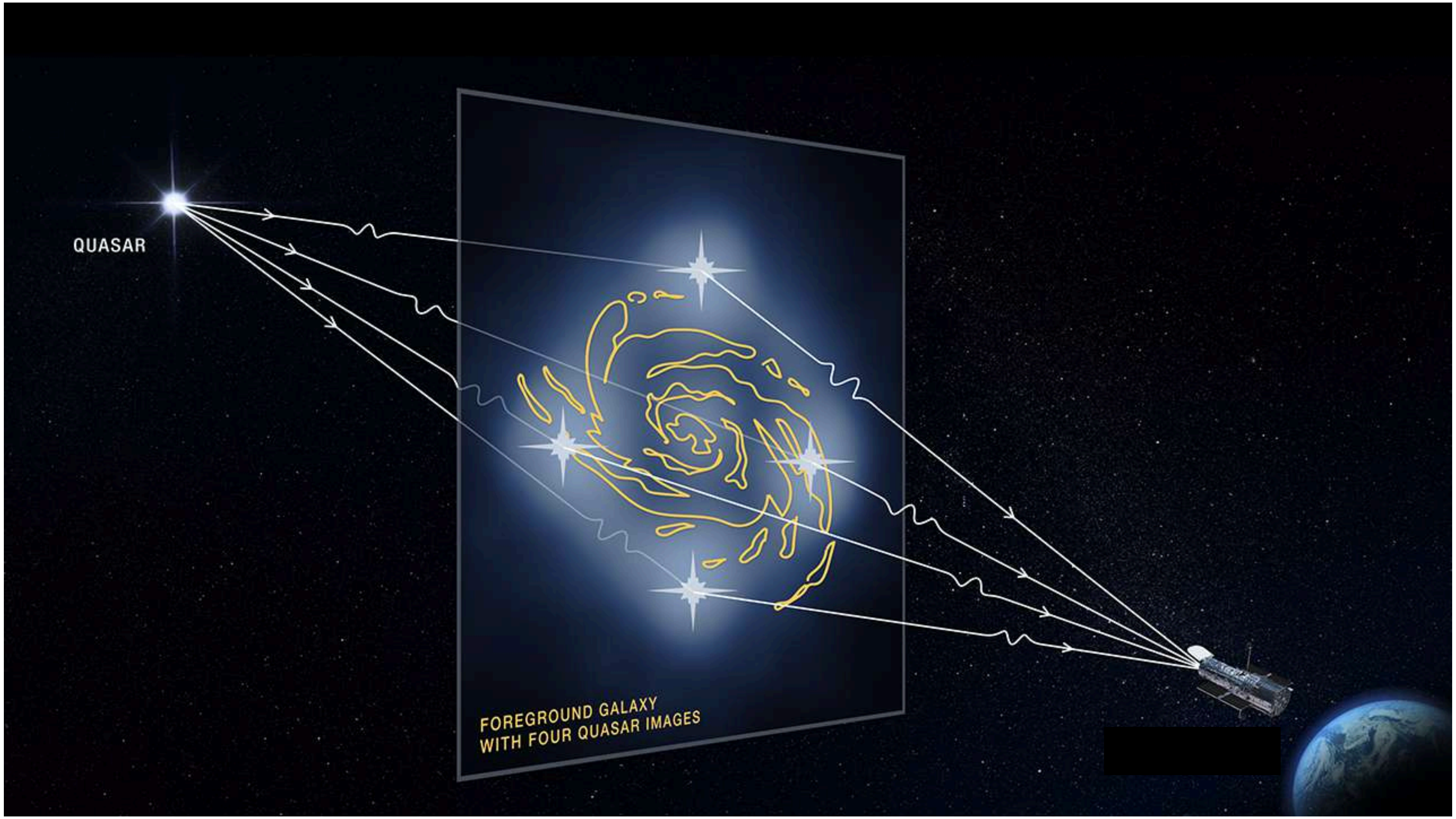

Detecting birefringence in lens system

Basu, Goswami, Schwarz, Y.U. (Phys. Rev. Lett. 21)

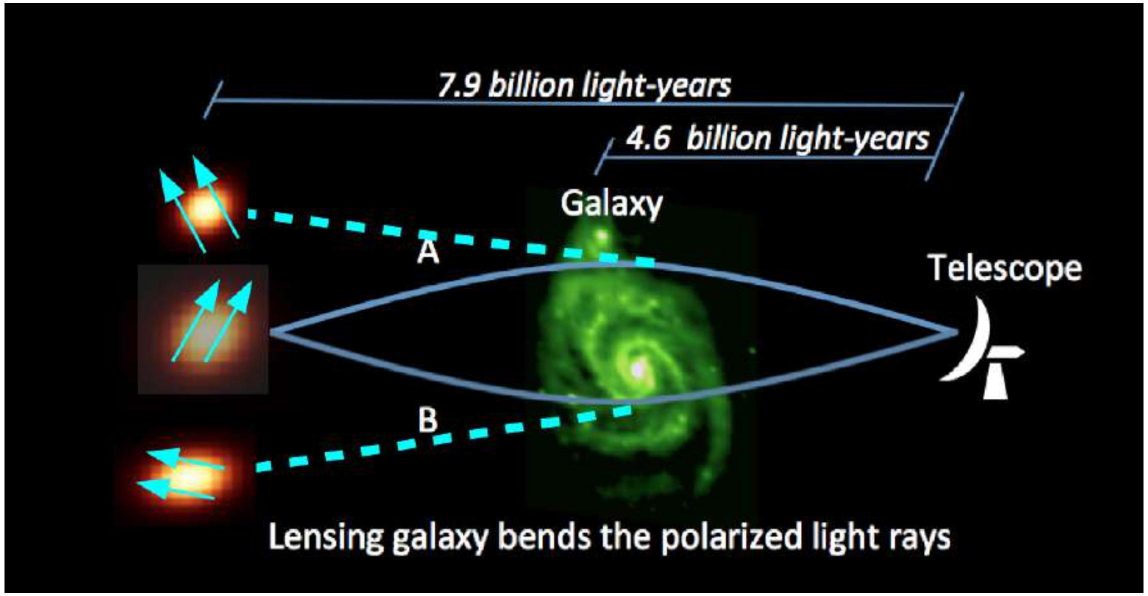

CLASS B1152+199

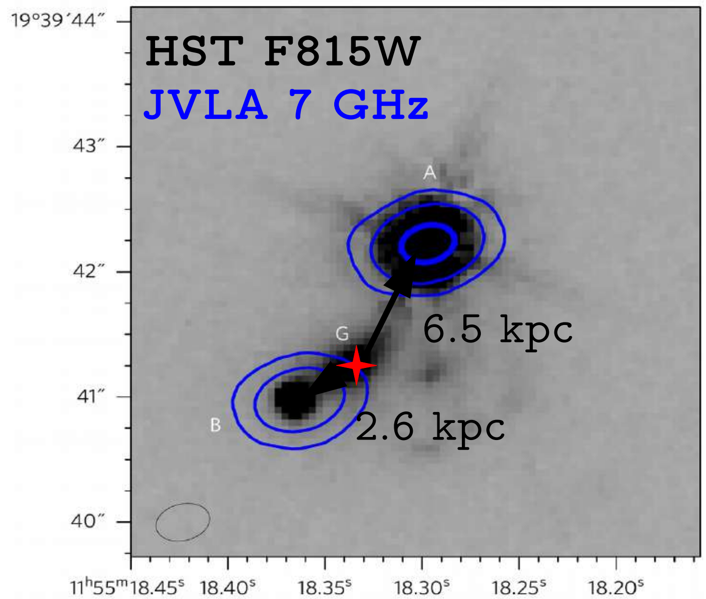

Mao et al. (Nature Astron. 17)

Differential birefringence in lensing system

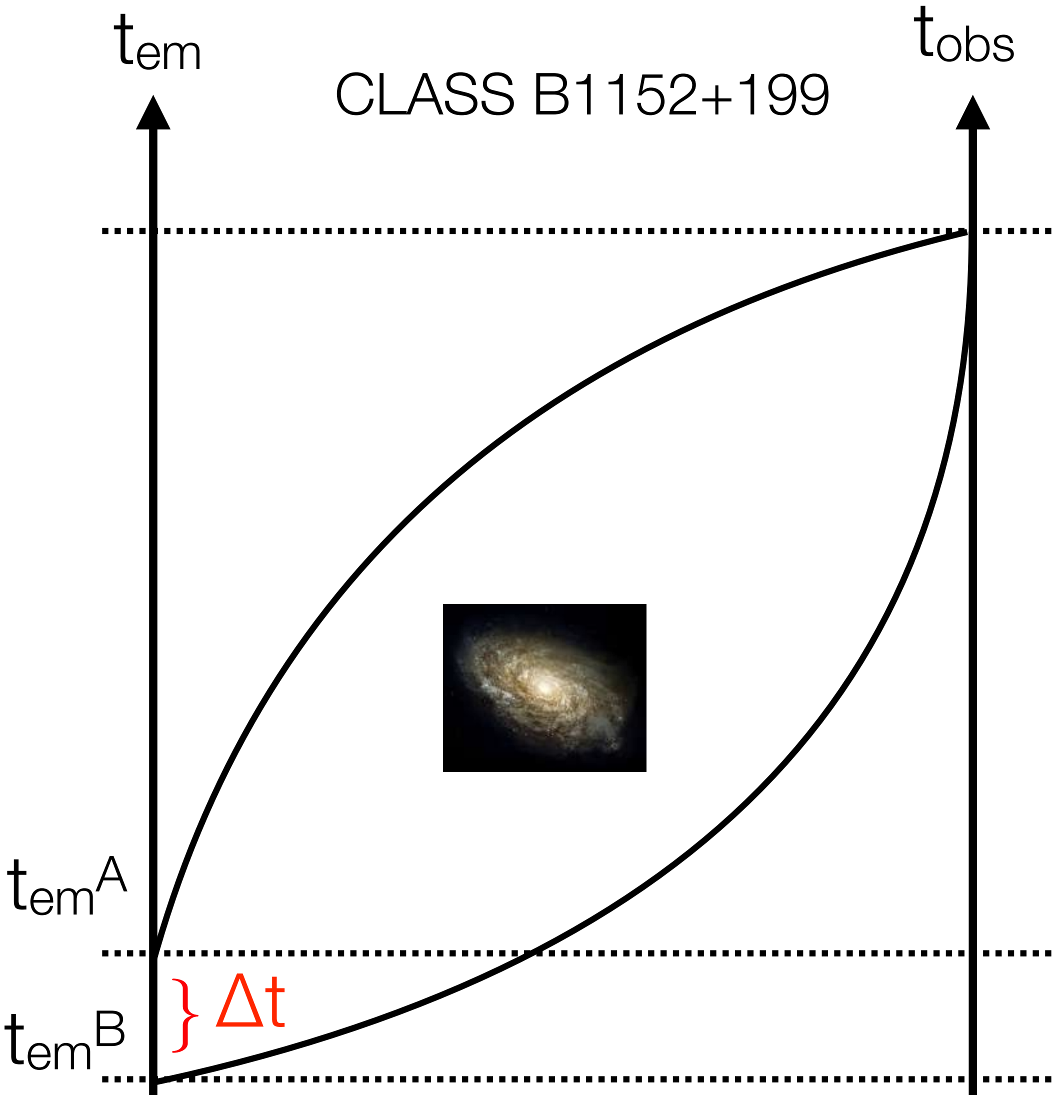

lens modeling
$\Delta t \sim 13$ days *Rusin et al. (02),*

Basu, Goswami, Schwarz, Y.U. (Phys. Rev. Lett. 21)

t_{obs}  (J)VLA

Birefringence for two images

$$\theta_{0\alpha} = \theta_{\rm qso} + \Delta\,\theta_{\rm a}^{\alpha} + \delta\,\theta_{\rm cal} \qquad \alpha = A, B$$

Differential Birefringence

$$\theta_{0,\mathrm{A}} - \theta_{0,\mathrm{B}} = \Delta\theta_{\mathrm{a}}^{\mathrm{A}} - \Delta\theta_{\mathrm{a}}^{\mathrm{B}}$$

$$\Delta\theta_a^{\alpha} = \frac{g_{a\gamma}}{2}\left[\phi(t_{\rm obs}, x^i_{\rm obs}) - \phi(t^{\alpha}_{\rm em}, x^i_{\rm em})\right]$$

$$= \frac{g_{a\gamma}\sqrt{2\rho_{\rm a}^{\rm em}}}{m_{\rm a}} \sin\left(\frac{m_{\rm a}\Delta t}{2}\right) \cos\left(\frac{m_{\rm a}(t_{\rm em}^{\rm A} + t_{\rm em}^{\rm B})}{2} + \delta_{\rm em}\right)$$

VLA monitoring of CLASS B1152+199

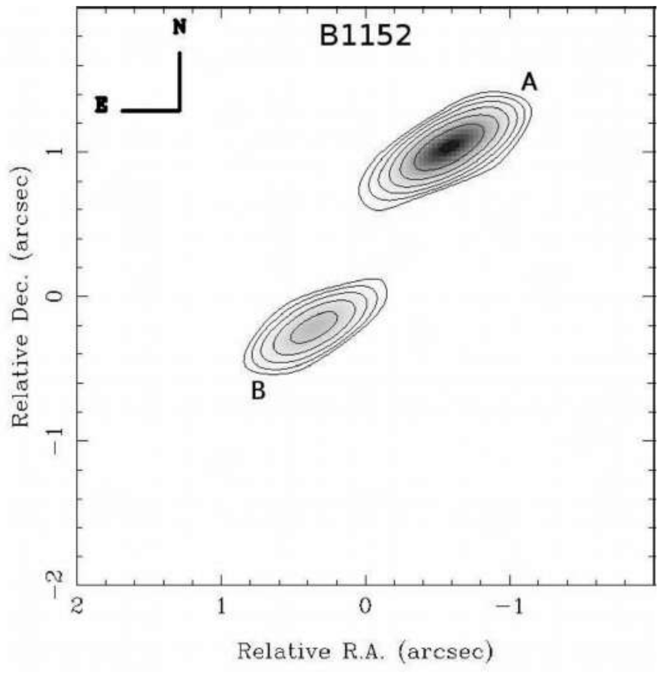

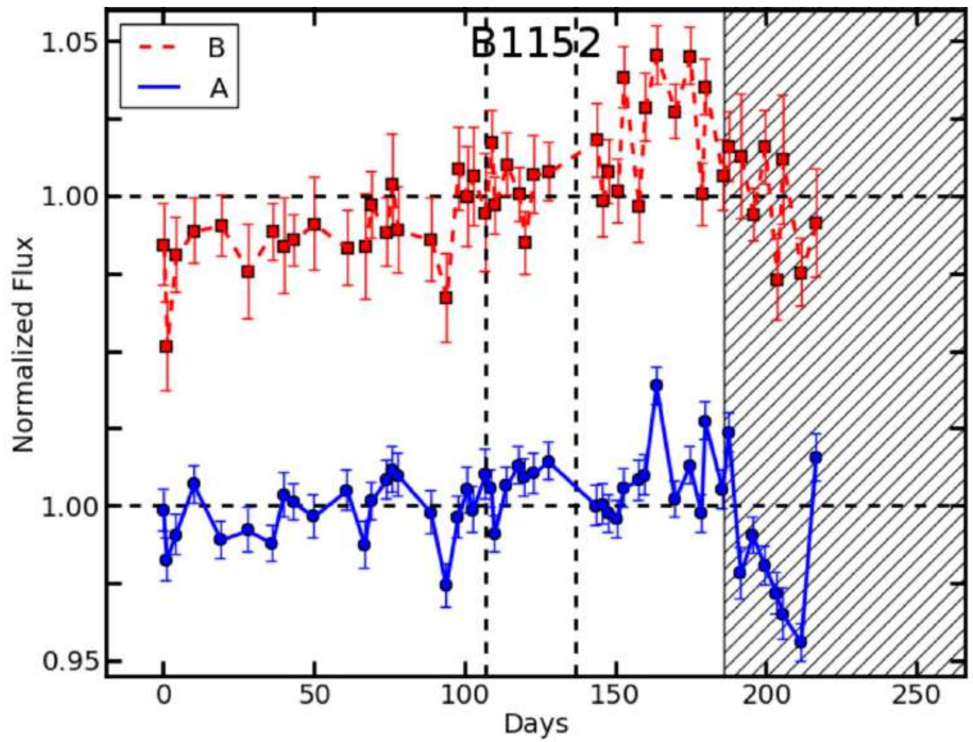

Rumbaugh et al. (2015) MNRAS

No evidence of AGN variability over 7 months (cadence ~3.5 days)

* Time variation is within the expected calibration error.

Contamination: Faraday effect

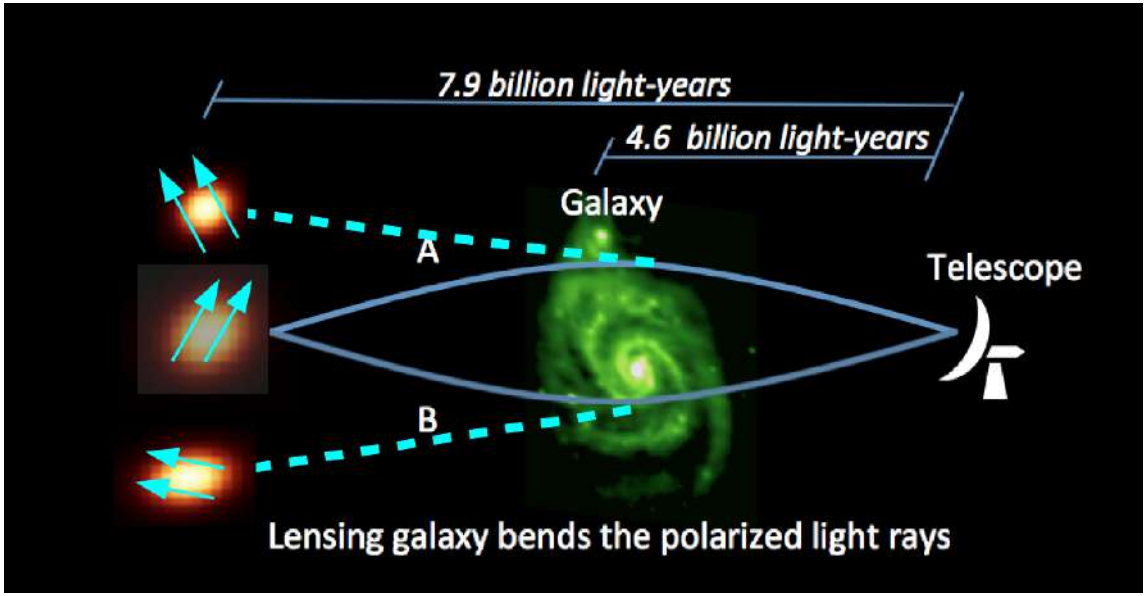

Faraday effect due to galactic/intergalactic B field.

$$\Delta\theta_{\text{Faraday}} \propto \text{RM}\,\lambda^2$$

⟶ Spectropolarimetry at cm wavelength to remove chrometric birefringence due to Faraday effect

Basu, Goswami, Schwarz, Y.U. (Phys. Rev. Lett. 21)

ALPs search from differential birefringence

Basu, Goswami, Schwarz, Y.U. (Phys. Rev. Lett. 21)

$$\theta_{0,\mathrm{A}} - \theta_{0,\mathrm{B}} = \frac{g_{\mathrm{a}\gamma}\sqrt{2\rho_{\mathrm{a}}^{\mathrm{em}}}}{m_{\mathrm{a}}} \sin\left(\frac{m_{\mathrm{a}}\Delta t}{2}\right) \cos\left(\frac{m_{\mathrm{a}}(t_{\mathrm{em}}^{\mathrm{A}} + t_{\mathrm{em}}^{\mathrm{B}})}{2} + \delta_{\mathrm{em}}\right)$$

$$\Delta\theta_{\mathrm{a,lens}} = 1.04^{+7.67}_{-5.59}\ \mathrm{deg}$$

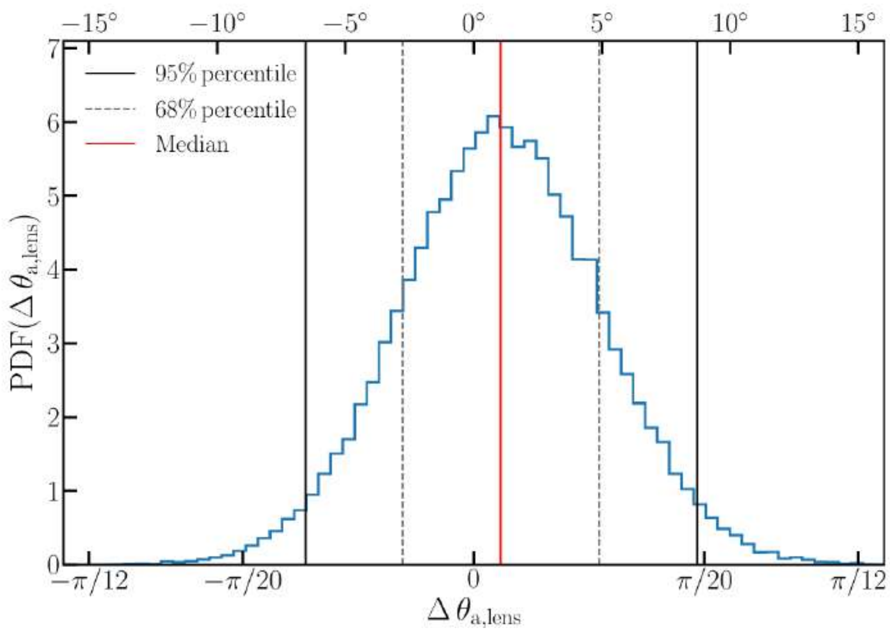

$\Delta t|_{@\mathrm{QSO}}$ = 13.3 days

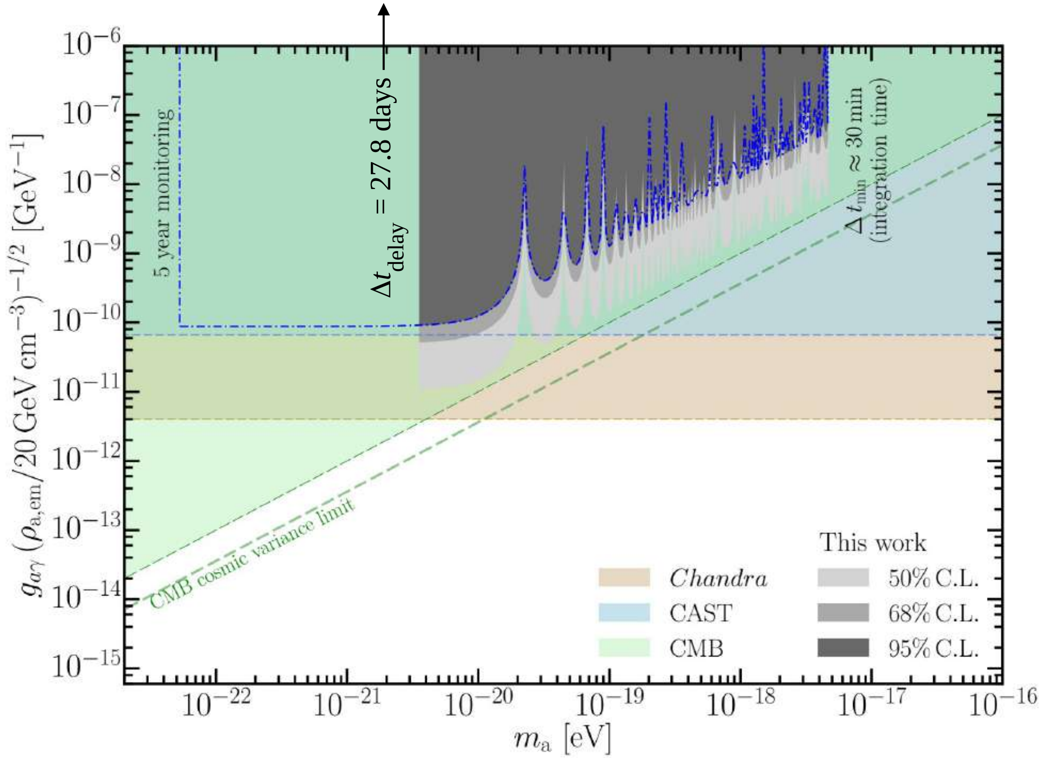

Observation proposal just submitted….

Selecting 5 out of 220 lensed AGNs.

Observing Application

Date:	
Proposal ID:	VLA/2021-06-041
PI:	Aritra Basu
Type:	Regular
Category:	High Redshift and Source Surveys
Total time:	21.55

Searching for axionlike particles using the JVLA and the VLBA

- Incl. lens system w/larger time delay

(Δt_{delay}=420 days)

- Longer monitoring

Square Kilometer Array (SKA)

SKA1 low

- 50MHz - 350 MHz
- 130,000 antennas
- max baseline 70 km

SKA1 mid

- 350MHz - 14 GHz
- 200 antennas
- max baseline 150 km

Improvement of sensitivity, speed of performing surveys, resolution

(of extensive sources)

Forecast on SKA1

<u>SKA1-mid</u>

10^5 strong lenses

if 5% is quasars

→ 5,000 systems

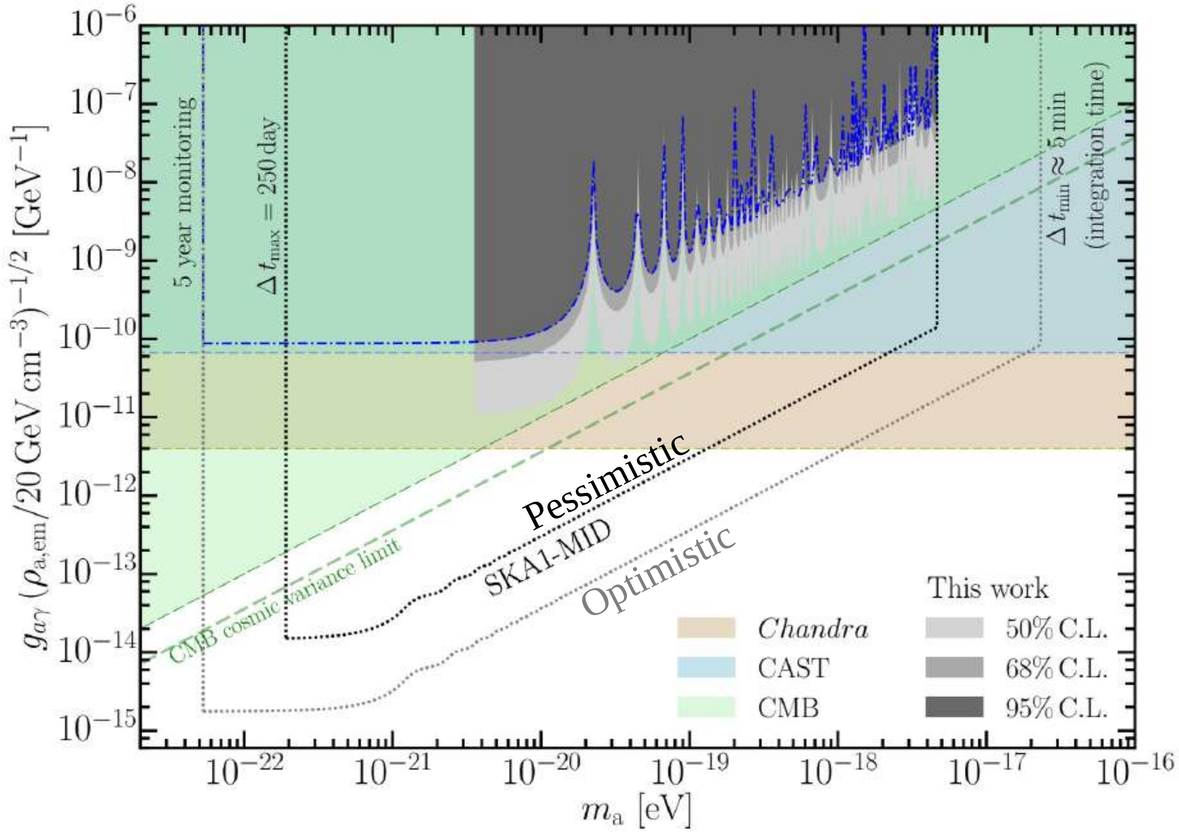

- Wider mass range

- (At least) 2 orders of magnitude improvement

Summary

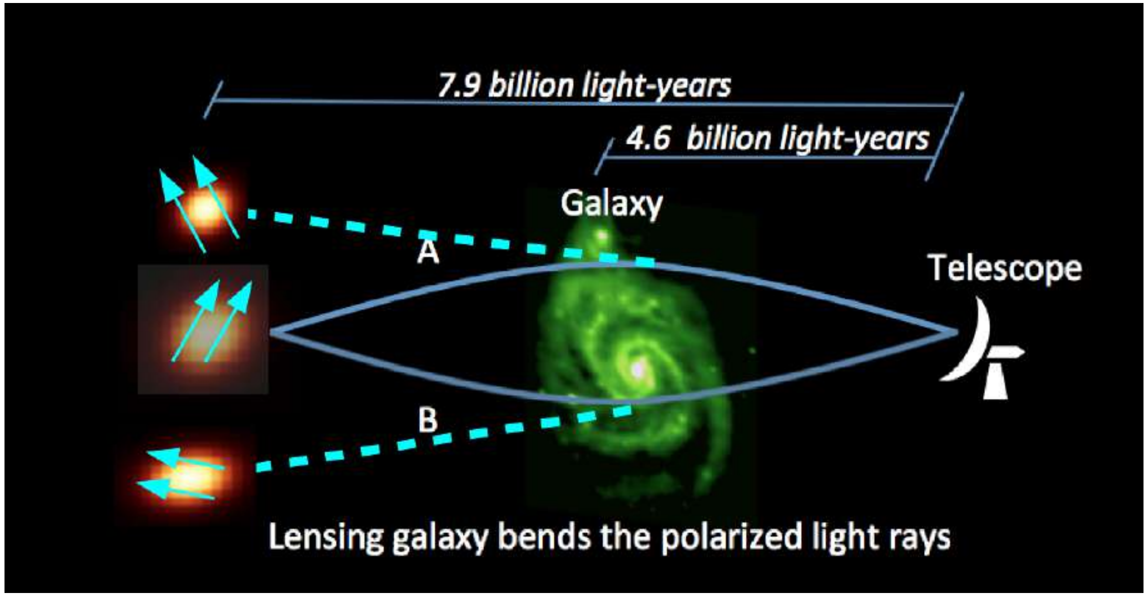

- Lensed quasars provide the cleanest tool to look for ULA DM.

- Lensed quasar CLASS B1152 + 199

$$g_{\alpha\gamma} < 9.2 \times 10^{-11}\ \mathrm{GeV}^{-1} \quad \text{for} \quad m_a < 3.6 \times 10^{-21}\ \mathrm{eV}.$$

Basu, Goswami, Schwarz, Y.U. (Phys. Rev. Lett. 21)

Supplement

Spectropolarimetry

CLASS B1152+199 via JVLA

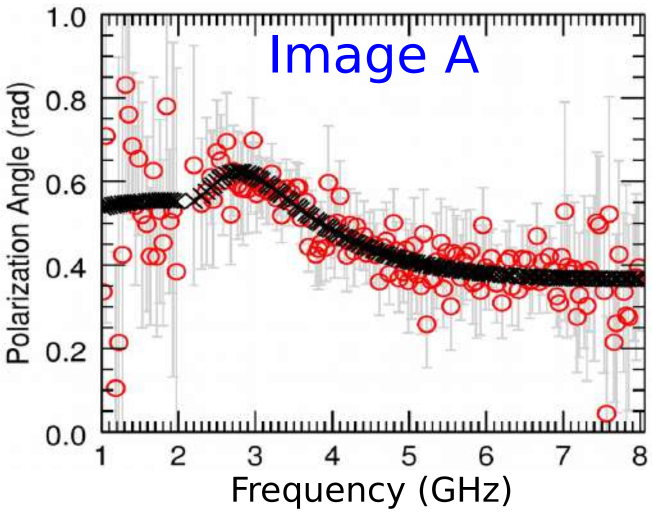

Extrapolated to $\lambda=0$ by applying Stokes *Q,U* fitting.

O'Sullivan et al., (2012), MNRAS
Pasetto, w/ Basu, et al. (2018), A&A

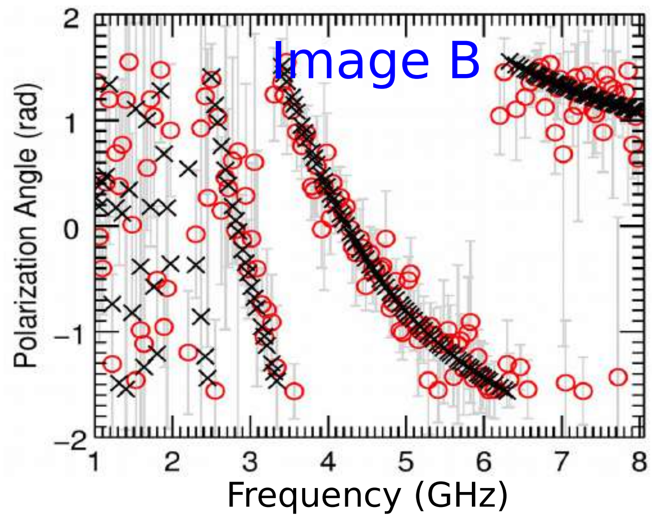

The background quasar undergoes Faraday rotation and depolarization in the lensing galaxy.

Lensing galaxy of B1152+199

Radio observation by VLBA

Rusin et al. (MNRS 02),

Precise optical astrometry by HST

<u>Mass modeling</u>

Scaled surface density

$$\kappa(x_1, x_2) = \frac{q}{(x_1^2 + x_2^2/f^2)^{\beta/2}},$$

bestfit

	$\beta = 0.8$	$\beta = 0.9$	$\beta = 1.0$	$\beta = 1.1$	$\beta = 1.2$
f	$0.787^{+0.024}_{-0.025}$	$0.755^{+0.029}_{-0.030}$	$0.719^{+0.034}_{-0.035}$	$0.677^{+0.040}_{-0.041}$	$0.627^{+0.046}_{-0.048}$
$\mathrm{PA_G}$	$-73.4^{+3.3}_{-3.6}$	$-76.3^{+3.6}_{-4.0}$	$-79.4^{+3.9}_{-4.2}$	$-82.6^{+4.2}_{-4.4}$	$-85.6^{+4.3}_{-4.4}$
Δt	28.3 ± 1.6	32.1 ± 1.8	35.9 ± 2.0	$39.7^{+2.3}_{-2.2}$	$43.4^{+5/2}_{-2.4}$
$A_{A,11}$	$+0.379^{+0.018}_{-0.017}$	$+0.430^{+0.021}_{-0.020}$	$+0.482^{+0.024}_{-0.022}$	$+0.533^{+0.026}_{-0.025}$	$+0.582^{+0.027}_{-0.026}$
$A_{A,12}$	$-0.273^{+0.011}_{-0.010}$	-0.284 ± 0.013	-0.290 ± 0.015	-0.292 ± 0.017	-0.292 ± 0.018
$A_{A,22}$	$+0.682^{+0.009}_{-0.010}$	$+0.762^{+0.011}_{-0.012}$	$+0.838 \pm 0.013$	$+0.910^{+0.014}_{-0.015}$	$+0.975^{+0.015}_{-0.016}$
$A_{B,11}$	$+0.247^{+0.054}_{-0.056}$	$+0.317^{+0.060}_{-0.062}$	$+0.396^{+0.066}_{-0.067}$	$+0.484 \pm 0.073$	$+0.580^{+0.078}_{-0.079}$
$A_{B,12}$	$-0.681^{+0.028}_{-0.027}$	$-0.792^{+0.033}_{-0.032}$	$-0.905^{+0.038}_{-0.037}$	$-1.021^{+0.042}_{-0.041}$	$-1.137^{+0.046}_{-0.045}$
$A_{B,22}$	$-0.356^{+0.097}_{-0.103}$	$-0.366^{+0.109}_{-0.116}$	$-0.357^{+0.119}_{-0.127}$	$-0.324^{+0.126}_{-0.134}$	$-0.265^{+0.131}_{-0.138}$
$\mathrm{PA_B}$	$+123.0^{+4.1}_{-3.9}$	$+126.1^{+4.3}_{-4.0}$	$+129.9^{+4.5}_{-4.2}$	$+134.5^{+4.8}_{-4.4}$	$+140.0^{+5.1}_{-4.7}$

* Different H_0 value is used in our analysis.

Birefringence on CMB

Fedderke et al. (19)

Inhomogeneous patches
(k/m >> 1)

$$\Delta\theta = \frac{g_{a\gamma}}{2}\left[\phi(t_{\rm obs}, x^i_{\rm obs}) - \phi(t_{\rm em}, \cancel{x^i_{\rm em}})\right]$$

decoupling

Surface of LSS ~ 10^4 yr >> Oscillation period ~ yr

For |f(t)| << 1 with $f(t) \equiv g_{\phi\gamma}\phi_0\cos(mt+\alpha)$

$$\begin{pmatrix} Q(\hat{\mathbf{n}},t) \\ U(\hat{\mathbf{n}},t) \end{pmatrix} = \boxed{\begin{pmatrix} 1 & -f(t) \\ f(t) & 1 \end{pmatrix}} \boxed{\begin{pmatrix} \langle Q(\hat{\mathbf{n}})\rangle \\ \langle U(\hat{\mathbf{n}})\rangle \end{pmatrix}}$$

$X_0 \to \langle X\rangle = J_0(g_{a\gamma}\phi_{\rm dec})X_0$

$J_0(x) \approx 1 - x^2/4$

$X = U, Q$

AC effect — Washout effect

Oscillation at observer — Smearing

Birefringence on CMB

BICEP/Keck collaboration(20)

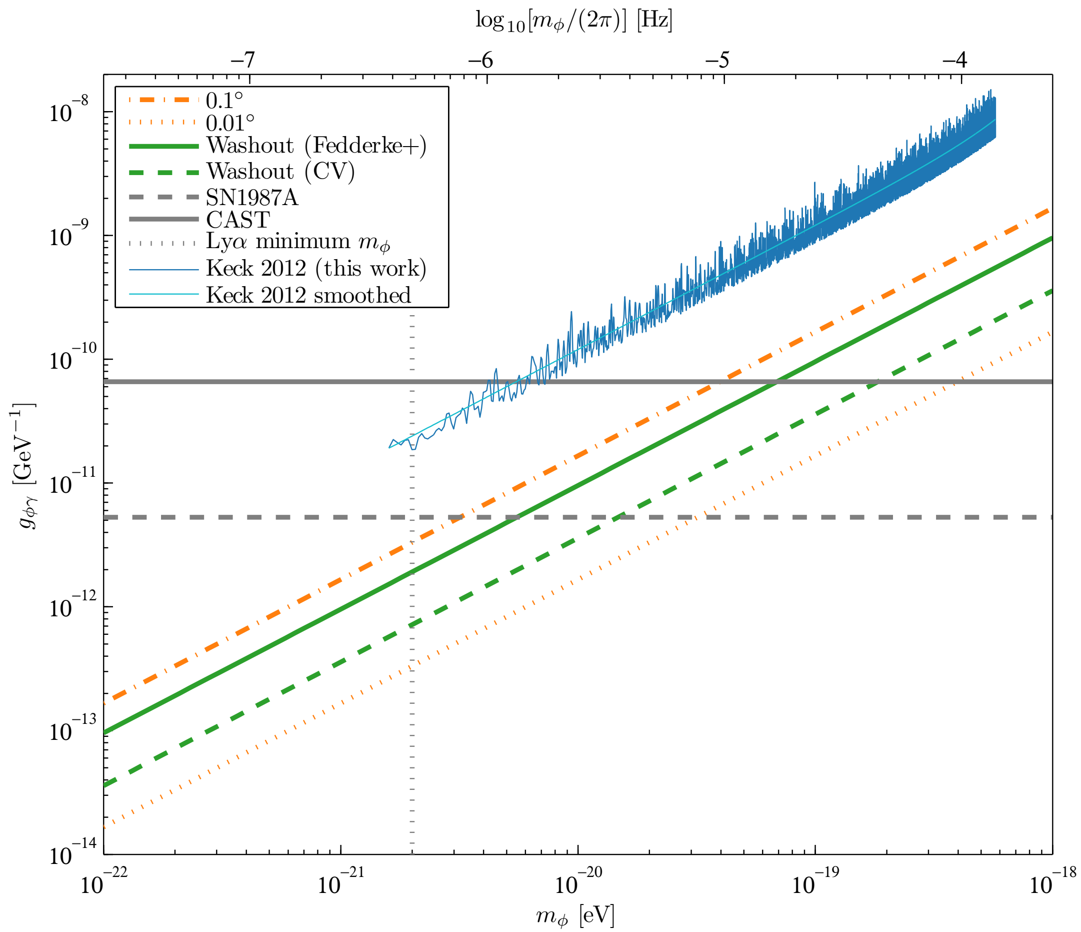

FIG. 6. Excluded regions in the mass-coupling parameter space for axion-like dark matter (cf. Fig. 3 in [15]). All constraints push the allowed regions to larger masses and smaller coupling constants, i.e., toward the bottom right of the figure. If the dark matter is assumed to consist entirely of axion-like particles, i.e., if $\kappa = 1$, then our constraints (blue) are immediately implied by Eq. 4 and the results of Fig. 5. A smoothed approximation is shown in cyan (Eq. 79). The orange dot-dashed and dotted lines show the constraints that would be achieved if the rotation amplitude were constrained to 0.1° and 0.01°, respectively. The green solid line shows the constraint set by Fedderke et al. [15] by searching for the washout effect (Sec. I) in publicly available *Planck* power spectra. The dashed green line shows the cosmic-variance limit for the washout effect. The dashed grey horizontal line shows the limit from searching for a gamma-ray excess from SN1987A [22]. The solid grey horizontal line is the limit set by the CAST experiment [21]. The dotted grey vertical line is a constraint on the minimum axion mass from observations of small-scale structure in the Lyman-α forest [26], though we note that several similar bounds have also been set by other considerations of small-scale structure [27, 28].

Protoplanetary disks

Slide from A. Basu

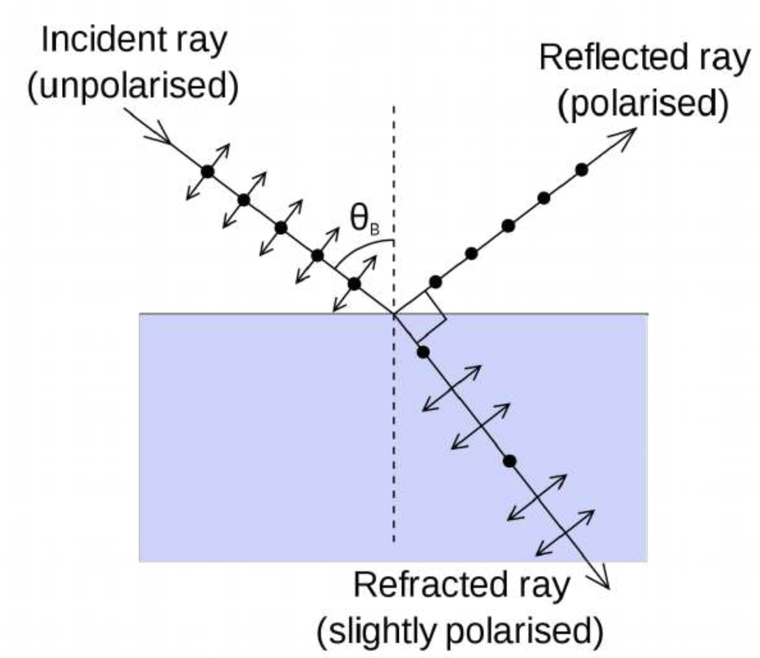

Scattering induces polarization in the perpendicular direction.

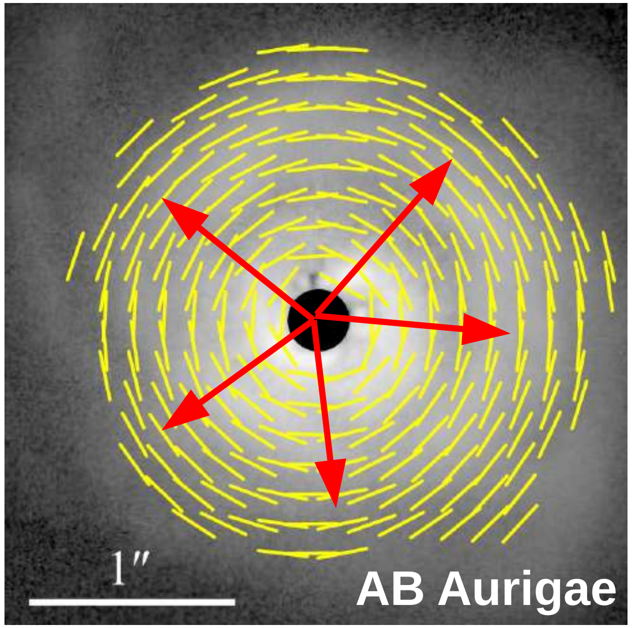

Hashimoto et al. (2011) ApJ

For thin disks, photon path is along the radial vector

⇒ Polarization perpendicular

Protoplanetary disks

Slide from A. Basu

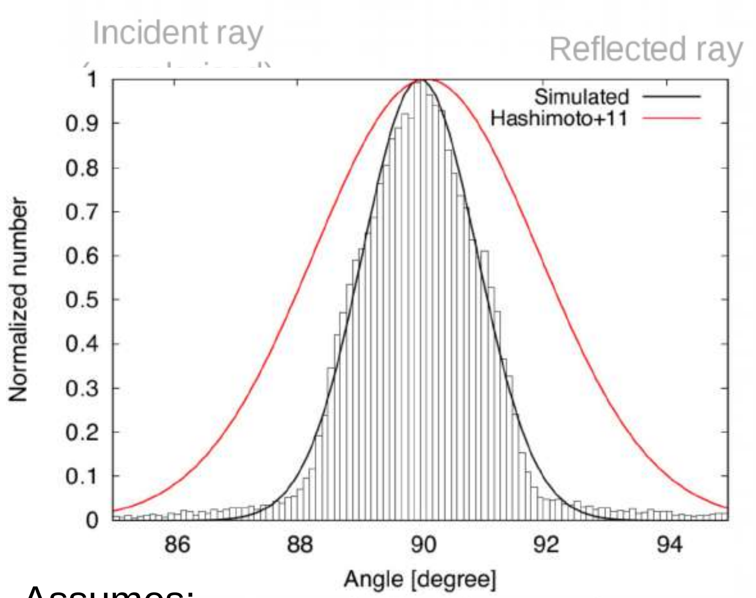

Assumes:

– Perfectly face-on orientation
– Thin disk

Non-detection limited by angle calibration and astrophysical modelling.

Fujita et al. (2019) PRL

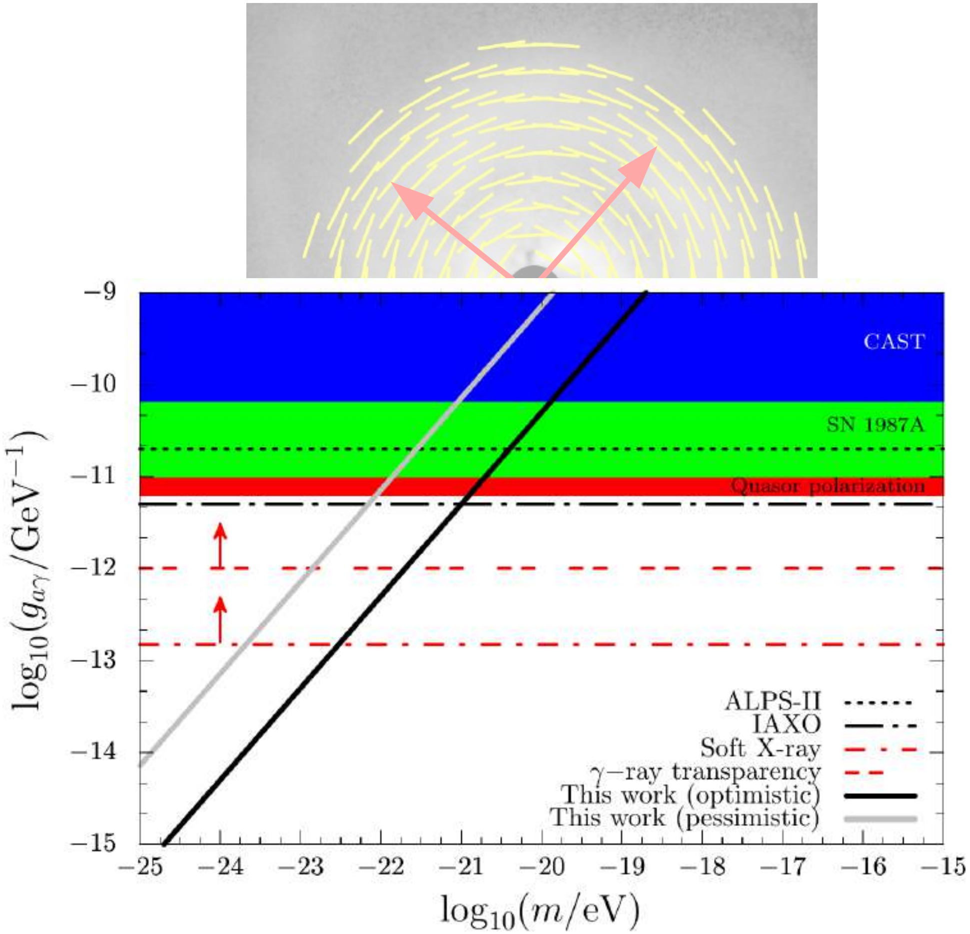

Subtlety of thin disk approx.

Montesinos et al. (ApJ 21, arXiv: 2102.02874)

AGN jet

Slide from A. Basu

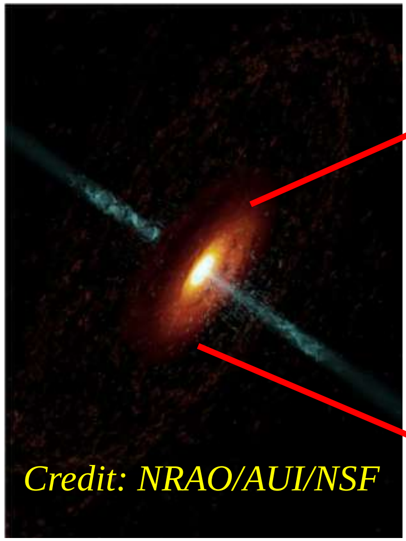

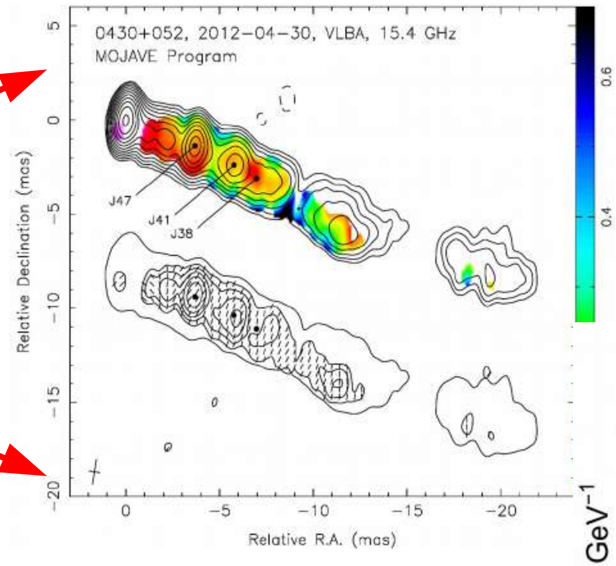

Ivanov et al. (2019) JCAP

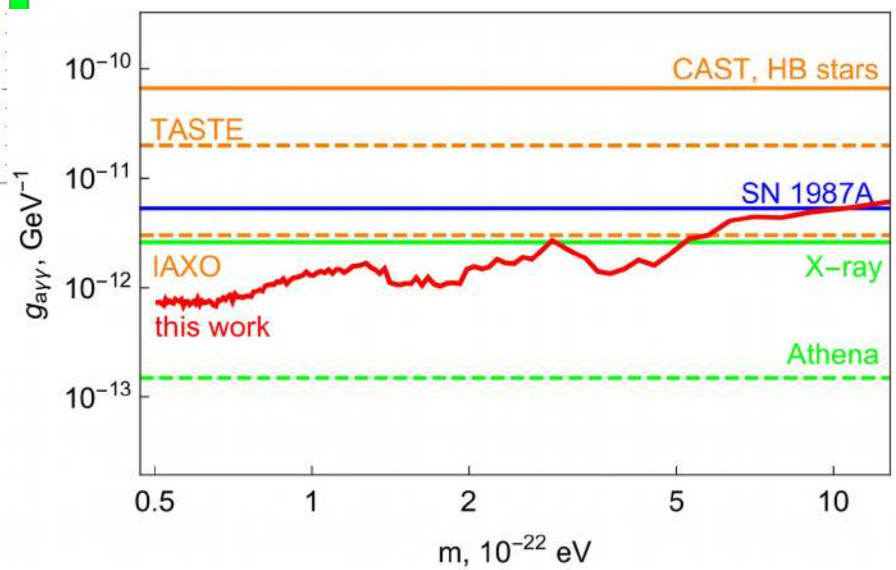

Non-detection limited by angle calibration,
astrophysics & instrument stability